Synthesis and Characterization of Silver (Core)/Layered Double Hydroxide (Shell) Nanoparticles

Woo Noh, Xiaodi Sun, Aishwarya Ramachandran, Colton Rearick, Sandwip K. Dey*

School for Engineering of Matter, Transport and Energy, Center for Interventional Biomaterials, Ira Fulton College of Engineering, Arizona State University, Tempe, AZ 85287, USA

Sandwip.dey@asu.edu

Abstract-**The development of metallic Silver (Ag) core and layered double hydroxide (LDH) shell nanoparticles (NPs) holds promise in nanomedicine. This drug delivery platform may induce simultaneous therapeutic actions, i.e., hyperthermia due to plasmon resonance of Ag and apoptosis due chemotherapeutic agent within LDH, as well as provide molecular imaging capability. Herein, for the first time, Ag (core)/(Mg^{2+}, Al^{3+})-LDH (shell) NPs are synthesized, and the results of characterization of the morphology, composition and surface plasmon resonance (SPR) of the core/shell NPs with varying shell thickness are reported. For the pure 45 nm Ag NP core, the wavelength for transverse SPR absorption was 395 nm, which red-shifted up to 430 nm at a LDH shell thickness of 15 nm. Additionally, the synthesis and characterization of the Ag nanorods are also presented. The observation of longitudinal SPR absorption in the near infrared range makes Ag nanorods a more appropriate core material.**

Keywords- Ag Core/LDH Shell Nanoparticles; Coprecipitation; Layered Double Hydroxide; Surface Plasmon Resonance; Theranostics

I. INTRODUCTION

Nanomedicine exploits the high potential of nanotechnology with the progressive understanding of molecular and cellular biology by using platforms having combined therapeutic and diagnostic attributes (i.e., theranostics) for medical benefits. To date, some drug-loaded polymeric liposomes have already gained FDA approval [1], but inorganic nanostructures are also making their mark [2]. Quantum dot, silica, and magnetic nanoparticle (NP)-based theranostics are now in various stages of preclinical and clinical development [3]. Another inorganic ceramic which holds promise in nanomedicine is the layered double hydroxide (LDH), based on the Hydrotalcite ($Mg_6Al_2(OH)_{16}CO_3{\cdot}4H_2O$) structure. Here, the positively charged cation hydroxide layers are rendered electrically neutral by electrostatically-bound anions. The space between the octahedral-cation (e.g., divalent Mg^{2+}, Co^{2+}, Zn^{2+} and trivalent Al^{3+}, $^{67}Ga^{3+}$, Fe^{3+}, Mn^{3+}, Gd^{3+} etc.) layers may be occupied by intercalated anions (e.g., nucleotides, fluorescent molecules, radio-labeled ATP, vitamins, DNA, and drugs), with water held in place via hydrogen bonding to the hydroxyls [4]. To date, one *in vivo* magnetic resonance imaging study [5] and a number of *in vivo* studies [6]-[10] using animal models to determine the pharmacokinetics, toxicity, transfection efficiency, and therapeutic efficacy of LDH, have been reported. In order for this LDH platform to compete with polymeric and other inorganic theranostics, it is important to demonstrate the potential for additional modalities with respect to therapy and imaging, while maintaining structural simplicity and ease of processing of 100-200 nm NPs [5]. For example, combination therapy may be accomplished by (i) an apoptosis-inducing, chemotherapeutic agent intercalated within the interlayer space of the LDH nanoshell, and (ii) hyperthermic ablation of cancer cells via surface plasmon resonance (SPR) absorption in the near infrared (NIR) region (650–900 nm) [11] by synthesizing a LDH shell on a noble metal core as core/shell nanoparticles. Since the former, i.e., insertion of chemotherapeutic agents in phase-pure LDH, has been amply demonstrated; this article reports a preliminary step towards the fulfillment of the latter goal.

Recently, a few methods for the syntheses of submicron, ceramic magnetic core/LDH shell, particles have been reported. A tedious layer by layer adsorption of commercially available LDH nanosheets onto large Fe_3O_4 core (500 nm) was used to synthesize submicron Fe_3O_4 core/(Mg^{2+}, Al^{3+})-LDH shell particles [12]. One post-synthetic mechanical processing method, such as ball milling, was used to reduce the particle size after the synthesis of micron-sized $MgFe_{1.03}O_{2.54}$ core/(Mg,Al)-LDH shell particles [13]. Another method for the synthesis of Fe_3O_4 core/(Mg^{2+}, Al^{3+})-LDH shell NPs was by the precipitation of a 10 nm thick LDH shell onto 220 nm Fe_3O_4 core, aggregated from primary particles of 10-15 nm [14]. In order to synthesize core/LDH shell nanoparticles with specific sizes, stability of the core NPs under LDH synthesis condition, minimization of homogeneous nucleation, uniformity of heterogeneous nucleation of LDH on the NP core, and control of LDH shell thickness are critical, and thus presents major challenges.

Herein, for the first time, the synthesis of spherical Ag (core)/LDH (shell) NPs using coprecipitation method without the need of any post-treatments, as well as the results of physico-chemical characterization are reported. The ultraviolet-visible (UV-vis) spectroscopy data indicate that for a given spherical Ag core diameter, a red-shift of the maximum wavelength (λ_{max}) for transverse SPR absorption takes place with increasing LDH shell thickness up to 15 nm [15]. However, the shift is not extended into the desired NIR region. In contrast, since bare Ag nanorods show SPR

absorption in the NIR region, it will perhaps be a more appropriate core to synthesize Ag (nanorod core)/LDH (shell) NPs for nanomedicine.

II. EXPERIMENTAL

All synthesis procedures and treatments were carried out at room temperature (25ºC), unless specified otherwise. All chemicals were purchased from Sigma (St. Louis, MO, USA) and used as received unless otherwise indicated.

A. Preparation of Silver Core Nanoparticles

A 10 ml solution of 0.25 mM $AgNO_3$ and 0.25 mM sodium citrate dihydrate was prepared. While vigorously stirring this solution, 600 µl of 0.01 M ice-cold $NaBH_4$ was added all at once. The color of the solution immediately changed to light yellow, indicating the formation of the seed solution; note, the seed solution was used within 12 hours since the Ag particles had a tendency to aggregate and to form a Ag thin film on the solution surface. This seed solution was used for the synthesis of Ag (core)/LDH (shell) NPs, as well Ag nanorods.

B. Synthesis of Ag (core)/LDH (shell) Nanoparticles

For coating the Ag NPs with the LDH shell, a 50 ml solution containing 3.33 mM $MgCl_2 \cdot 6H_2O$, and 1.67 mM $AlCl_3 \cdot 9H_2O$, and 50 ml of 0.01 M NaOH base solution were simultaneously added to a 3-neck flask containing 50 ml of previously prepared Ag seed solution. Following the constant pH synthesis route, the pH was maintained at 10 while adding the salt and basic solutions. After aging for different durations (3, 6, 12 h), the solutions were centrifuged at 7000 rpm for 30 min. The supernatants were removed, and the Ag (core)/LDH (shell) NPs were re-dispersed in deionized water.

C. Synthesis of Ag Nanorods

Five sets of 0.1 M cetyltrimethylammonium bromide (CTAB) solutions of 10 ml were prepared. These solutions were heated to 40ºC to dissolve the CTAB and then cooled to room temperature. Next, 0.25 ml of 0.01 M $AgNO_3$ and 0.5 ml of 0.1 M ascorbic acid were added to each CTAB set. Then, various amounts of Ag seed solutions (i.e., 1.0, 0.5, 0.2, 0.1 and 0.05 ml) were added to the sets. Finally, 0.1 ml of 1 M NaOH solution was added to each set. Within 2 min of NaOH addition, the color changed from red to either brown or green depending on the concentration of Ag seed solution, and signaling a change in the aspect ratio. After aging for 1 hour, the solutions were centrifuged at 4000 rpm for 30 min. The supernatants (containing mostly small spheres and platelets) were removed, and Ag nanorods of various aspect ratios in different sets were re-dispersed in deionized water. The aspect ratio of the Ag nanorods increased with decreasing volume of Ag seed solution added.

D. Characterization

The morphology and particle size of Ag (core)/LDH (shell) NPs are examined by the field emission scanning electron microscopy (FESEM; XL30 ESEM-FEG), which are further corroborated with transmission electron microscopy (HRTEM; JEOL JEM-2010F TEM with an electron acceleration voltage of 200 KeV and analytical capability) bright field images. To prevent surface charging, the NPs were coated with 20 nm of gold by sputtering. The particle size and size distribution were also determined by dynamic light scattering (DLS; DynaPro MS/X, Protein Solutions Inc.). The crystallographic information of the Ag NPs and Ag (core)/LDH (shell) phases were collected using powder X-ray diffraction (XRD; Rigaku D/Max-IIB instrument with Cu-K_α radiation, λ = 0.154059 nm) in 2θ range of 8°-90°. The Ag (core)/LDH (shell) nanostructures were confirmed by TEM in the bright field imaging mode. In addition, the elemental composition of the core/shell NPs was spatially mapped by energy dispersive X-ray spectroscopy (EDX) to confirm the formation of the LDH shell on the Ag core. Moreover, the morphology and composition of synthesized Ag nanorods were determined by TEM and EDX. Finally, the plasmon resonance frequencies of the Ag (core)/LDH (shell) NPs and Ag nanorods were determined by ultraviolet-visible spectroscopy (UV-Vis; Perkin Elmer Lambda 18) as a function of LDH shell thickness, and aspect ratio, respectively.

III. RESULTS AND DISCUSSION

In order to synthesize Ag (core)/LDH (shell) NPs via heterogeneous coprecipitation [16], aggregation of Ag NPs (<50 nm) and homogeneous nucleation must be averted. Note, prior to the heterogeneous nucleation of LDH, Ag NPs were electrostatically stabilized via the negative surface charge of the citrate layer. First, the aggregation Ag NPs occurs below pH 4.6 (isoelectric point of citrate-stabilized NPs) [17]. Second, it was observed that Ag NPs transformed into aggregates when LDH salt solution was mixed with the Ag seed solutions because of an increase in the ionic strength. Due to electrostatic affinity, both Mg^{2+} and Al^{3+} cations stripped the charged citrate ligands away from the Ag NPs' surface, thereby rendering the unprotected Ag NPs towards aggregation. Third, it was found that high supersaturation condition favored homogeneous nucleation of LDH. Therefore, the optimized condition for the formation of the LDH shell on Ag NP core was the coprecipitation of a 50 ml solution containing 3.33 mM $MgCl_2 \cdot 6H_2O$, and 1.67 mM $AlCl_3 \cdot 9H_2O$ in the presence of Ag NPs seeds following a constant pH (~10) route under low supersaturation condition (see the experimental section).

The morphology and particle size of heterogeneous LDH in the form of Ag (core)/LDH (shell) NPs were characterized by FESEM, as shown in Figure 1a. The particles exhibited a monodisperse size distribution with diameter ~50 nm. The size and size distribution of Ag (core)/LDH (shell) NPs, determined by DLS (data not shown), corroborated the FESEM and TEM data (given below). In contrast, the homogeneously precipitated discoidal LDH NPs (shown in Figure 1b) had a much larger diameter ~145 nm, despite the identical concentration and volume of LDH precursors used during their (i.e., Ag (core)/LDH (shell) NPs and LDH NPs) syntheses. The remarkable differences in shape and particle size emanate

from the differences in the nucleation and growth mechanism between seed-mediated coprecipitation of core/shell NPs and homogeneous coprecipitation of LDH NPs. In the former case, the total surface area and the large number of spherical Ag NPs offer plenty of heterogeneous nucleation sites. Since the activation energy barrier for heterogeneous nucleation is much lower than for homogeneous nucleation [16], the LDH shells preferentially nucleate and grow on the spherical Ag NPs, resulting in a large number of narrowly-distributed, core/shell nanoparticles of much smaller size. Also, under the optimized reaction condition of low supersaturation, the homogeneous nucleation of LDH NPs is minimized in the presence of Ag nuclei.

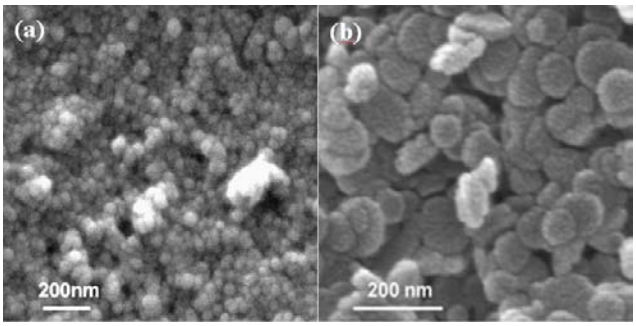

Figure 1 SEM images of (a) Ag (core)/LDH (shell) nanoparticles and (b) homogeneous LDH nanoparticles

The crystallinity of the Ag NPs (Figure 2a) and Ag (core)/LDH (shell) NPs (Figure 2b) were confirmed by XRD; the characteristic diffraction peaks of pure Ag and LDH were indexed and in agreement with past work on LDH [18]. With the experimental LDH d_{003} spacing of 0.793 nm (2θ = 11.15°), and published data on the thickness of the Brucite layer of ~ 0.48 nm [19], the gallery height (or interlayer spacing) is found to be ~0.313 nm. This implies that the intercalated species are a mixture of chloride (from precursor) and carbonate (from atmosphere) ions [4], [20], and in agreement with the EDX data (shown later). Identification of the peaks between 2θ of 37-40° (Figure 2c), shows that the Ag (111) and LDH (012) peaks overlap. Based on these XRD patterns, although it can be inferred that Ag and LDH phases coexist, it does not provide conclusive evidence of core/shell structures.

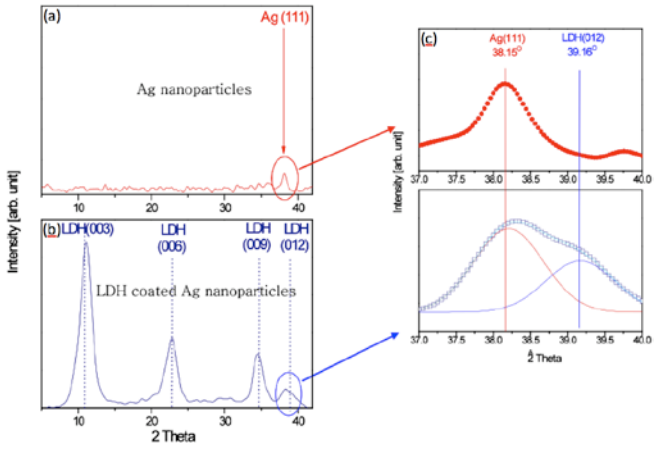

Figure 2 Powder XRD patterns of (a) pure Ag NPs, (b) Ag (core)/LDH (shell) NPs, and (c) magnified data in the 2θ = 37-40° range

Figure 3 illustrates TEM images of Ag (core)/LDH (shell) NPs, and spatially dependent EDX data; the high magnification image shows a Ag core (~45 nm) coated with a thin LDH shell (~10 nm). Moreover, the EDX data are indicative of distinct compositional transitions as the probe is scanned outward from the center of the Ag NP core, i.e., the Ag signal peak diminishes while the LDH component-peaks (Mg, Al, C, Cl and O) are enhanced, clearly indicating that LDH shell surrounds the Ag core.

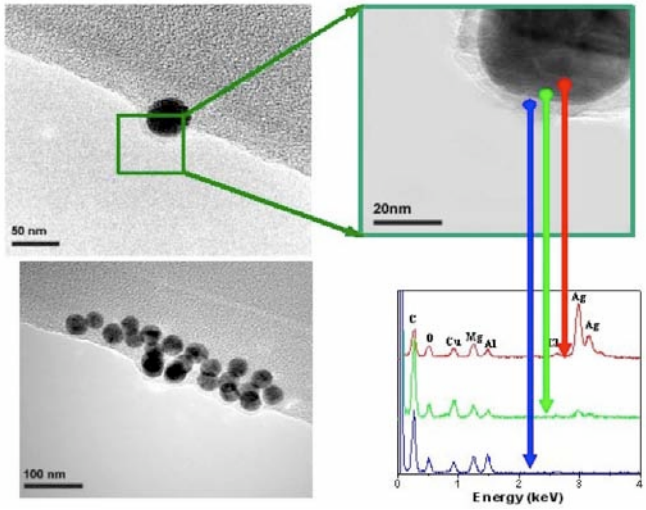

Figure 3 TEM images of spherical Ag (core)/LDH (shell) NPs with spatially-dependent EDX data

Both Ag NPs and various core/shell NPs have been intensively studied for their SPR properties [21], [22]. The SPR should arise when the incident photon frequency is resonant with the collective oscillations of the conduction electrons in the metal NP. From Mie theory, the magnitude of the extinction cross-section, comprising of the scattering and absorption components, as well as the wavelength (λ_{max}) corresponding to its peak at SPR, should depend on the size (core and shell), shape, NP spacing, and dielectric properties of core and shell [23]-[25]. Interestingly, if thickness of LDH shell or the size and aspect ratio of Ag cores can be varied, the Ag-LDH may be readily tuned for maximum absorption (i.e., hyperthermic ablation) or for maximum scattering (i.e., NIR imaging by confocal reflectance microscopy or optical coherence tomography) [26], [27]. Since the eventual target for this study is hyperthermic ablation [28]-[30], the focus here is on a size regime (<50 nm) of the spherical Ag core, where dipole plasmon absorption is by far the dominant contributor to the extinction cross-section [31].

Recent reports on the control of LDH shell thickness in core/shell inorganic structures include the tedious layer by layer adsorption LDH nanosheets onto large Fe_3O_4 cores (500 nm) [12], and post-synthetic ball milling in $MgFe_{1.03}O_{2.54}$ (core)/(Mg^{2+}, Al^{3+})-LDH (shell) [13]. In the current study, the shell thickness was found to be proportional to the (i) aging time (3, 6, 12 h), (ii) the quantity of 5 mM precursor salt solution, and (iii) inverse initial Ag NP density (either using 0 and 50 ml of Ag seed solution). Note, the latter methodology was the most reliable and controllable since the thickness of the LDH shell on the Ag core could be readily tuned within a few nanometers.

Figure 4 illustrates UV-vis spectroscopy data on the effects of the LDH shell thickness of spherical Ag (core)/LDH (shell) NPs; shell thicknesses (10, 12, and 15 nm) being controlled by various aging durations (3, 6 and 12 hr). For the Ag NP core, λ_{max} for transverse SPR is at 395 nm, and with increasing thickness of the LDH shell, λ_{max} red-shifts up to ~430 nm for a shell thickness of 15 nm. However, these shifts are not sufficient and fall far below the targeted NIR range (800 nm).

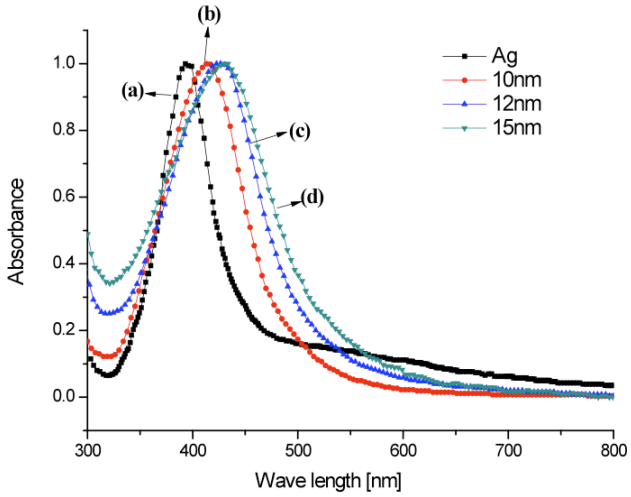

Figure 4 Absorption spectra by UV-Vis spectroscopy as a function of LDH shell thickness on Ag core.: (a) Ag NPs, (b) core/shell NPs with 10 nm shell thickness, (c) core/shell NPs with 12 nm shell thickness, and (d) core/shell NPs with 15 nm shell thickness

Silver nanorods with various aspect ratios were also synthesized (see the Experimental section). Just as gold (Au) nanorods [32], bare Ag nanorods, with varying aspect ratio that increased with decreasing volume of seed solution, gave promising results. Figure 5 shows a bright-field TEM image and EDX data for specific Ag nanorods of 90-110 nm in length and 20-30 nm in diameter.

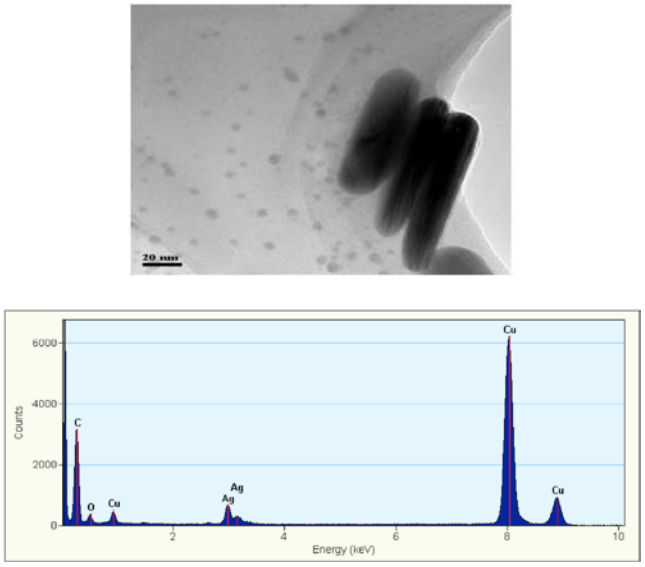

Figure 5 TEM bright-field image (top) of Ag nanorods and corresponding EDX data (bottom)

As depicted in Figure 6, the λ_{max} for longitudinal SPR resonance of these nanorods gradually shifts towards longer wavelengths with increasing aspect ratios; well into the NIR range. Also note that λ_{max} for both transverse and longitudinal SPRs are observed in the Ag nanorods, with the dominance of longitudinal resonance with increasing aspect ratio. Additionally, since the relative contribution of scattering to the total cross section increases, the longitudinal plasmon resonance broadens [31].

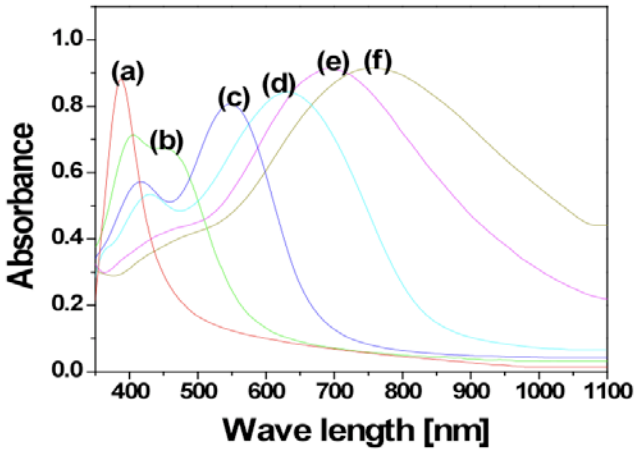

Figure 6 Absorption spectra by UV-Vis spectroscopy as a function of the aspect ratio of Ag nanorods synthesized with different amounts of seed solution. (a) Ag NP seeds, (b) 1000 µl, (c) 500 µl, (d) 200 µl, (e) 100 µl, and (f) 50 µl

IV. CONCLUSION

The present work was a preliminary step towards the eventual goal of achieving simultaneous hyperthermia and chemotherapy, as well as molecular imaging of cancer cells using the nanostructured Ag-LDH platform. Here, a simple approach for synthesizing mono-dispersed spherical Ag (core)/LDH (shell) NPs without the need for any post-synthesis treatments has been presented. The core/shell NPs and Ag nanorods were characterized by FESEM, XRD, DLS, TEM, EDX, and UV-vis spectroscopy. In the spherical Ag (core)/LDH (shell) NPs, dramatic increases in the shell thickness will be required to bring the transverse λ_{max} for SPR into the NIR region, but with the potential for NP aggregation. Alternatively, the lack of λ_{max}-shift in spherical systems can be mitigated by the use of Ag nanorod cores of appropriate aspect ratio. The consequent cylindrical-shaped Ag nanorod (core)/LDH (shell) NPs, with varying LDH shell thickness and chemotherapeutic loading capacity, could potentially become a competitive and multimodal theranostic platform.

ACKNOWLEDGEMENTS

SKD acknowledges financial support from the National Cancer Institute, National Institutes of Health (1R21CA133618), National Science Foundation (CBET-0829128), and ASU Foundation's Women & Philanthropy (WZ91010). The authors acknowledge and deeply appreciate the useful discussions with Professor Kaushal Rege of Chemical Engineering and Dr. Vinay Nagaraj of the Biodesign Institute at Arizona State University (ASU), and are grateful to Dr. Thomas Groy, Dr. Paul Westerhoff, and Dr. Karl Weiss of ASU for assistance with XRD, DLS, and TEM, respectively.

REFERENCES

[1] O. C. Farokhzad, and R. Langer, "Nanomedicine: Developing smarter therapeutic and diagnostic modalities," *Adv. Drug Deliver. Rev.*,vol. 58, pp. 1456-1459, Dec. 2006.

[2] H. C. Huang, S. Barua; G. Sharma, S. K. Dey, and K. Rege, "Inorganic nanoparticles for cancer imaging and therapy," *Journal of Controlled Release*, vol. 155, pp. 344-357, Nov. 2011.

[3] R. F. Service, "Nanotechnology: Nanoparticle Trojan Horses Gallop from the lab into the clinic," *Science*, vol. 330, pp. 314-315, Oct. 2010.

[4] S. K. Dey, and R. Sistiabudi, "Ceramic nanovector based on layered double hydroxide: attributes, physiologically relevant compositions and surface activation," *Mater. Res. Innov.*, vol. 11, pp. 108-117, Sep. 2007.

[5] A. Flesken-Nikitin, I. Toshkov, J. Naskar, K. M. Tyner, R. M. Williams, W. R. Zipfel, E. P. Giannelis, and A. Y. Nikitin, "Toxicity and biomedical imaging of layered nanohybrids in the mouse," *Toxicol. Pathol.*, vol. 35, pp. 804-810, Oct. 2007.

[6] S. J. Choi, J. M. Oh, and J. H. Choy, "Safety aspect of inorganic layered nanoparticles: Size-dependency in vitro and in vivo," *J. Nanosci. Nanotechno.* vol. 8, pp. 5297-5301, Oct. 2008.

[7] S. Y. Kwak, W. M. Kriven, M. A. Wallig, and J. H. Choy, "Inorganic delivery vector for intravenous injection," *Biomaterials*, vol. 25, pp. 5995-6001, Dec. 2004.

[8] M. Del Arco, E. Cebadera, S. Gutierrez, C. Martin, M. J. Montero, V. Rives, J. Rocha, and M. A. Sevilla, "Mg, Al layered double hydroxides with intercalated indomethacin: Synthesis, characterization, and pharmacological study," *J. Pharm. Sci.*, vol. 93, pp. 1649-1658, Jun. 2004.

[9] F. P. Bonina, M. L. Giannossi, L. Medici, C. Puglia, V. Summa, and F. Tateo, "Diclofenac-hydrotalcite: In vitro and in vivo release experiments," *Appl. Clay Sci.*, vol. 41, pp. 165-171, Oct. 2008.

[10] M. Silion, M. I. Popa, G. Lisa, and D. Hritcu, "New hybrid compounds containing intercalated Ciprofloxacin into layered double hydroxides: Synthesis and characterization," *Rev. Roum. Chim.*, vol. *53*, pp. 827, Sep. 2008.

[11] P. Cherukuri, E. S. Glazer, and S. A. Curleya, "Targeted hyperthermia using metal nanoparticles," *Adv. Drug Deliver. Rev.*, vol. 62, pp. 339-345, Mar. 2010.

[12] L. Li, Y. J. Feng, Y. S. Li, W. R. Zhao, and J. L. Shi, "Fe_3O_4 Core/Layered Double Hydroxide Shell Nanocomposite: Versatile Magnetic Matrix for Anionic Functional Materials," *Ange. Chem. Int. Edit.*, vol. 48, pp. 5888-5892, Jul. 2009.

[13] H. Zhang, D. K. Pan, K. Zou, J. He, and X. Duan, "A novel core-shell structured magnetic organic-inorganic nanohybrid involving drug-intercalated layered double hydroxides coated on a magnesium ferrite core for magnetically controlled drug release," *J. Mater. Chem.*, vol. 19, pp. 3069-3077, Mar. 2009.

[14] D. K. Pan, H. Zhang, T. Fan, J. G. Chen, and X. Duan, "Nearly monodispersed core-shell structural Fe_3O_4@DFUR-LDH submicro particles for magnetically controlled drug delivery and release," *Chem. Commun.*, vol. 47, pp. 908-910, 2011.

[15] A. Otto, "Excitation of nonradiative surface plasma waves in Silver by method of frustrated total reflection," *Z. Phys.*, vol. 216, pp. 398-410, 1968.

[16] D. A. Porter, and K. E. Easterling, *Phase Transformation in Metals and Alloys*, 2nd ed., Ed. UK: Chapman & Hall, 1996, Chapter. 4.

[17] S. H. Brewer, W. R. Glomm, M. C. Johnson, M. K. Knag, and S. Franzen, "Probing BSA binding to citrate-coated gold nanoparticles and surfaces," *Langmuir*, vol. 21, pp. 9303-9307, Sep. 2005.

[18] R. Chitrakar, Y. Makita, A. Sonoda, and T. Hirotsu, "Synthesis of a novel layered double hydroxides $[MgAl_4(OH)_{12}](Cl)_2{\cdot}2.4H_2O$ and its anion-exchange properties," *J. Hazard. Mater.*, vol. 185, pp. 1435-1439, Jan. 2011.

[19] R. Allmann, "Crystal structure of Pyroaurite," *Acta Crystall. B-Stru.*, vol. B 24, pp, 972-977, 1968.

[20] S. Tezuka, R. Chitrakar, A. Sonoda, K. Ooi, and T. Tomida, "Studies on selective adsorbents for oxo-anions. Nitrate ion-exchange properties of layered double hydroxides with different metal atoms," *Green Chem.*, vol. 6, pp. 104-109, Feb. 2004.

[21] T. R. Jensen, M. D. Malinsky, C. L. Haynes, and R. P. Van Duyne, "Nanosphere lithography: Tunable localized surface plasmon resonance spectra of silver nanoparticles," *Journal of Physical Chemistry B*, vol. 104, pp. 10549-10556, Nov. 2000.

[22] J. L. Lyon, D. A. Fleming, M.B. Stone, P. Schiffer, and M. E. Williams, "Synthesis of Fe oxide core/Au shell nanoparticles by iterative hydroxylamine seeding," *Nano Letters*, vol. 4, pp. 719-723, Apr. 2004.

[23] R. W. Wood, "On a remarkable case of uneven distribution of light in a diffraction grating spectrum," *Philos. Mag.*, vol. 4, pp. 396-402, Jul. 1902.

[24] C. F. Bohren, and D. R. Huffman, *Absorption and Scattering of Light by Small Particles*, Ed. Germany: John Wiley & Sons, 1983.

[25] P. K. Jain, K. S. Lee, I. H. El-Sayed, and M. A. El-Sayed, "Calculated absorption and scattering properties of gold nanoparticles of different size, shape, and composition: Applications in biological imaging and biomedicine," *J. Phys. Chem. B*, vol. 110, pp. 7238-7248, Apr. 2006.

[26] L. R. Hirsch, R. J. Stafford, J. A. Bankson, S. R. Sershen, B. Rivera, R. E. Price, J. D. Hazle, N. J. Halas, and J. L. West, "Nanoshell-mediated near-infrared thermal therapy of tumors under magnetic resonance guidance," *Proc. Natl. Acad. Sci. USA*, vol. 100, pp. 13549-13554, Nov. 2003.

[27] C. Loo, A. Lin, L. Hirsch, M. H. Lee, J. Barton, N. J. Halas, J. West, and R. Drezek, "Nanoshell-enabled photonics-based imaging and therapy of cancer," *Technol. Cancer Res. T.*, vol. 3, pp. 33-40, Feb. 2004.

[28] S. J. Oldenburg, J. B. Jackson, S. L. Westcott, and N. J. Halas, "Infrared extinction properties of gold nanoshells," *Appl. Phys. Lett.*, vol. 75, pp. 2897-2899, Nov. 1999.

[29] R. Weissleder, "A clearer vision for in vivo imaging," *Nat. Biotechnol.*, vol. 19, pp. 316-317, Apr. 2001.

[30] M. L. J. Landsman, G. Kwant, G. A. Mook, and W. G. Zijlstra, "Light-absorbing properties, stability, and spectral stabilization of Indocyanine Green," *J. Appl. Physiol.*, vol. 40, pp. 575-583, 1976.

[31] R. D. Averitt, S. L. Westcott, and N. J. Halas, "Linear optical properties of gold nanoshells," *J. Opt. Soc. Am. B*, vol. 16, pp. 1824-1832, Oct. 1999.

[32] S. Link, M. B. Mohamed, and M. A. El-Sayed, "Simulation of the optical absorption spectra of gold nanorods as a function of their aspect ratio and the effect of the medium dielectric constant," *J. Phys. Chem. B*, vol. 103, pp. 3073-3077, Apr. 1999.